Competitive binding predicts nonlinear responses of olfactory receptors to complex mixtures

Vijay Singh[a,b], Nicolle R. Murphy[c], Vijay Balasubramanian[a,b,1,2], and Joel D. Mainland[c,d,2]

[a]Computational Neuroscience Initiative, University of Pennsylvania, Philadelphia, PA 19104; [b]Department of Physics, University of Pennsylvania, Philadelphia, PA 19104; [c]Monell Chemical Senses Center, Philadelphia, PA 19104; and [d]Department of Neuroscience, University of Pennsylvania, Philadelphia, PA 19104

Edited by Katherine Nagel, New York University, New York, NY, and accepted by Editorial Board Member John R. Carlson March 27, 2019 (received for review August 2, 2018)

In color vision, the quantitative rules for mixing lights to make a target color are well understood. By contrast, the rules for mixing odorants to make a target odor remain elusive. A solution to this problem in vision relied on characterizing receptor responses to different wavelengths of light and subsequently relating these responses to perception. In olfaction, experimentally measuring receptor responses to a representative set of complex mixtures is intractable due to the vast number of possibilities. To meet this challenge, we develop a biophysical model that predicts mammalian receptor responses to complex mixtures using responses to single odorants. The dominant nonlinearity in our model is competitive binding (CB): Only one odorant molecule can attach to a receptor binding site at a time. This simple framework predicts receptor responses to mixtures of up to 12 monomolecular odorants to within 15% of experimental observations and provides a powerful method for leveraging limited experimental data. Simple extensions of our model describe phenomena such as synergy, overshadowing, and inhibition. We demonstrate that the presence of such interactions can be identified via systematic deviations from the competitive-binding model.

olfaction | sensory coding | receptor biophysics | olfactory receptor neurons | odor mixtures

In the field of flavors and fragrances, methods for mixing odorants to make a target odor are largely the domain of experts who have undergone years of training. Their expertise comes from examining historical formulas as well as extensive trial-and-error work, and their methods are primarily qualitative. In vision, by contrast, the rules for mixing lights to make a target color are quantitative and well developed. These rules are derived from a detailed characterization of human color perception and its relation to cone photoreceptor spectral sensitivities (1–3). Indeed, known tuning curves relate the wavelength of light to the responses of three types of cone photoreceptors. These input-response functions are then incorporated into models that extrapolate from the responses to single wavelengths to an arbitrary mixture of wavelengths. Finally, these receptor responses are used to predict color perception.

Here, we propose an analogous approach for characterizing the response of receptors to single odorants and modeling the responses to combinations of odorants. Simple summation models are widely used (4–8), but fail to account for several observed interactions, such as suppression, masking, hyperadditivity (or synergy), hypoadditivity (or compression), configural perception, and overshadowing. The wide variety of mixture interactions suggests that a simple model would struggle to explain experimental results, but here we show that a minimal biophysical description of odorant–receptor interaction incorporating the simplest possible nonlinearity, namely competition between molecules for the binding site, can successfully predict the responses of many mammalian odor receptors to complex molecular mixtures. Previously, Rospars et al. (9) found that responses of olfactory receptor neurons to some simple binary mixtures were largely consistent with a similar model and could display both hyper- and hypoadditivity. Related results for binary mixtures have also been reported for neurons in the accessory olfactory system (10) and in the antennal lobes of *Drosophila* (11) and locust (12). Cruz and Lowe (13) subsequently developed a biophysically motivated version of this model and applied it to glomerular imaging. Marasco et al. (14) extended this work to allow different odorants to have different Hill coefficients and thus different degrees of binding cooperativity, which allowed for the phenomena of synergy and inhibition, although a biophysical motivation was lacking. Meanwhile, Reddy et al. (15) developed biophysically motivated models of the phenomenon of antagonism in receptor neurons.

Here, we present two key steps forward. First, we collect receptor data for a large set of odors and show that our competitive-binding model largely accounts for the response of olfactory receptors to complex mixtures of up to 12 odorants. Second, we develop a systematic strategy to identify additional nonlinear interactions among odorants and receptors that go beyond the effects of competitive binding. Our approach is rooted in basic biophysics. For example, the extended models consider consequences of known phenomena like receptors with multiple binding sites, facilitation by already bound odorants, noncompetitive inhibition, and heterodimerization of odorant molecules in mixture and predict effects such as synergy, antagonism (16), and overshadowing (17) in receptor responses. Such phenomena are reported in studies of human olfactory

Significance

Predicting the response of the olfactory system to natural odors, typically complex mixtures of many molecules, is a major challenge. Here, we show that the nonlinear mixing response of many mammalian olfactory receptors is largely explained by the competition of molecules for binding sites. The resulting model of receptor responses provides a significant step toward synthesizing odors by adding "odor primaries" just as arbitrary colors can be created from mixtures of three primary colors.

Author contributions: V.S., V.B., and J.D.M. designed research; V.S., N.R.M., V.B., and J.D.M. performed research; V.S., V.B., and J.D.M. analyzed data; and V.S., V.B., and J.D.M. wrote the paper.

The authors declare no conflict of interest.

This article is a PNAS Direct Submission. K.N. is a guest editor invited by the Editorial Board.

Data deposition: Data collected and used in this study are available on Open Science Framework (https://osf.io/aj29q/).

[1]To whom correspondence should be addressed. Email: vijay@physics.upenn.edu.

[2]V.B. and J.D.M. contributed equally to this work.

This article contains supporting information online at www.pnas.org/lookup/suppl/doi:10.1073/pnas.1813230116/-/DCSupplemental.

Published online April 18, 2019.

perception (18), but their origin is unknown. We hypothesize that such nonlinear effects, previously assumed to be of neural origin, may already have a contribution from interactions at the level of the receptor.

Results

Competitive-Binding Model. The response of a receptor to an odor can be modeled in terms of the binding and unbinding of odorant molecules to and from the binding site. We assume that only one molecule can attach to a binding site at a time, leading to competition. In the presence of many odorants, the outcome of competition depends on three parameters: the concentration of the individual molecules, the efficacy with which the molecule activates the receptor, and the affinity of the molecule for the binding site.

We modeled the response of a receptor to the binding of an odorant as a two-step process (*SI Appendix*, *Competitive binding model*) (19). Such models have widely been used to study kinetics of chemical and biological systems starting with Michaelis and Menten in 1913 (20–24). In the first step, the molecule binds reversibly to the binding site. At this stage, the bound receptor can either dissociate, giving back the odorant and the unbound receptor, or reversibly go to an active state. The transition to the active state is the second step. In the active state, the odorant–receptor complex elicits a detectable response. In our experiments, this response is measured using a luciferase reporter in a cell-based assay (25).

In this competitive-binding (CB) model, the response of a receptor $F(\{c_i\})$ to a mixture of N odorants with concentrations represented by $\{c_i\}$ is given by (derivation in *SI Appendix*, *Competitive binding model*)

$$F(\{c_i\}) = \frac{F_{\max}\sum_{i=1}^{N}\frac{e_i c_i}{EC50_i}}{\left(1+\sum_{i=1}^{N}\frac{c_i}{EC50_i}\right)}. \quad [1]$$

Here, $EC50_i$ is the concentration at which the response is half of the maximum for odorant i, e_i is the efficacy of the receptor for odorant i, and $F_{\max}$ parameterizes the total receptor concentration and overall response efficiency (*SI Appendix*).

CB Model Predicts Receptor Responses to Mixtures. We used a heterologous assay to measure receptor responses to three monomolecular odorants (eugenol, coumarin, and acetophenone) known to broadly activate mammalian odor receptors (26). Dose–response curves were measured for 15 receptors (e.g., Fig. 1*A*) by stimulating the receptors across the full range of concentrations allowed by our assay ([0,0.3 mM]; *Materials and Methods*; see ref. 27 for deposited data). These 15 receptors were then stimulated with 21 mixtures (12 binary, 9 ternary) of eugenol, coumarin, and acetophenone (*Materials and Methods* and *SI Appendix*, Table S1) with concentrations now chosen to avoid receptor saturation.

We first fitted the CB model to the dose–response data for individual odorants ($n = 1$ in Eq. **1**). We selected parameters to minimize the root-mean-square error between predictions and measurements (*SI Appendix*, Table S4) weighted by the experimental SD (*Materials and Methods*; example in Fig. 1*A*, further details in *SI Appendix*, *Model parameter estimation*). The parameters that best reproduced the single-odorant data were then used to predict the response to odorant mixtures (Fig. 1 *B* and *C*).

For most receptors (12 of 15), the root-mean-square error (rmse) (*Materials and Methods* and *SI Appendix*, Fig. S1) was low (median below 0.1) and small relative to the observed response (median of rmse/observed response = 0.16) and compared with the experimental SDs (median rmse/SD = 1.2). (See *Extensions of the Model* for the remaining 3 receptors.) The results are consistent with the hypothesis that the receptor response is generated by the CB model (chi-square test, null hypothesis that CB model generates the responses is not rejected, $P > 0.999$; details in *SI Appendix*). We also tested whether the CB model predictions are robust to parameter variations that keep the predicted dose–response curves within 1 SD of the best fit (*SI Appendix*, Fig. S1).

Next we compared the rmse of the CB model to that of a summation model where responses were predicted to be linear sums of responses to individual odorants in the dose–response analysis (*Material and Methods*). Such summation models have previously been applied to the responses of olfactory sensory neurons and in the olfactory bulb (4–7). In addition, the human psychophysics

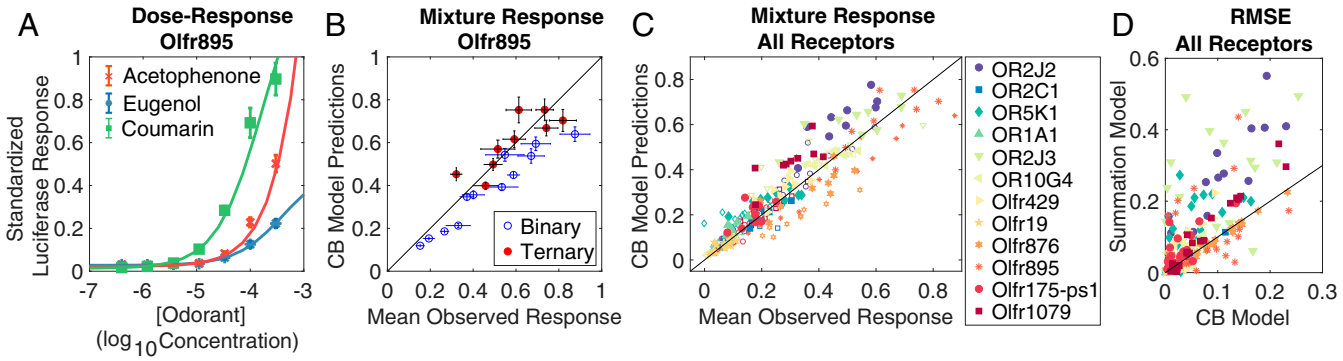

Fig. 1. A competitive-binding model predicts olfactory receptor response to binary/ternary mixtures. (*A*) Response of receptor Olfr895 to individual odorants. Markers show mean experimental response ±1 SD. Solid curves show the competitive-binding (CB) model with parameters chosen to minimize the error E_i defined as the root-mean-square error between model and data weighted by experimental SDs (main text and *SI Appendix*, *Model parameter estimation*). (*B*) Response of Olfr895 to binary and ternary mixtures. CB model predictions are plotted against experimental responses averaged over four replicates. The black diagonal line is the unit slope line. Horizontal bars represent ±1 SD. Vertical error bars are SD over mixture predictions for 300 randomly chosen sets of model parameters constrained so that the error E_i was lower than $\lceil E_i^{min} \rceil$, where E_i^{min} is the error for the best-fit parameters and $\lceil\rceil$ is the ceiling function (*SI Appendix*, *Standard deviation in CB model predictions*). In general this amounts to picking random parameter sets such that the model dose–response curves lie within 1 SD of the experimental mean (*SI Appendix*, *Materials and Methods*). (*C*) Response of 12 olfactory receptors from humans and mice to binary and ternary mixtures (CB model vs. average experimental responses: binary mixture responses, open symbols; ternary mixture responses, solid symbols; diagonal line, unit slope line). For these 12 receptors, the median root-mean-square error (rmse) was below 0.1. (See *SI Appendix*, Fig. S1 for alternative measures of prediction error.) (*D*) rmse of summation model plotted vs. the rmse of CB model. rmse of summation model lies above the diagonal unit slope line for most mixtures, indicating that the summation model predictions are worse compared with those of the CB model.

literature frequently assumes a summation model as the default for the perceived intensity of binary mixtures (8, 28). We found that the rmse for the CB model was lower than that for the summation model (Fig. 1*D*). This improvement occurred even though mixture concentrations were chosen to lie in an approximately "linear" regime that avoided saturation. We also tested whether the CB model predictions were better than the summation model predictions in terms of other measures of prediction error (*SI Appendix*, Fig. S2 *A* and *B*). The median CB model predictions lie within ∼15% of the actual magnitude of the response to individual mixtures. These results confirm the model's accuracy.

To further challenge the model, we studied the response of olfactory receptors to mixtures that were more comparable in complexity to natural odors, which typically have about 3–40 perceptually important components (29, 30). We focused on mouse receptor Olfr168, which responds to a large number of odorants (26). From the data in Saito et al. (26) we identified 12 odorants that evoked responses in this receptor (*Materials and Methods*). Similar to the procedure above, we first fitted the dose–response measurements for all 12 odorants to get the best parameters for the receptor (Fig. 2*A* and *SI Appendix*, Table S5; see ref. 27 for deposited data). Then, we used the competitive-binding model to predict receptor responses to mixtures with all 12 odorants present in diverse proportions (*Materials and Methods* and Fig. 2*B*). Trivially, a combination of many odors at a moderate concentration will activate receptors to saturation. To avoid this, we chose concentrations of the mixture components such that the receptor activation in response to the full mixture was above threshold and below saturation. The model predicted the receptor responses to such complex mixtures very well (Olfr168: CB median rmse = 0.16). The results are consistent with the hypothesis that the receptor response is generated by the CB model (chi-square test, null hypothesis that CB model generates the responses is not rejected, $P > 0.999$; details in *SI Appendix*). The CB model also outperformed a summation model of mixture response by more than 10-fold (Olfr168: summation median rmse = 1.91). Thus, for complex odor mixtures such as those occurring naturally, our nonlinear competitive-binding model presents a dramatic improvement over a summation model.

We wondered whether the specificity of receptor–odorant interactions determines model accuracy or whether good prediction results from simply fixing responses to be sigmoidal in the response range of a typical receptor. To test this, we compared the CB model to a shuffled model where, instead of using the specific dose–response curves of mixture components, we selected dose–response parameters randomly from all such parameters available in our dataset (*Materials and Methods*) and averaged the prediction error over 300 such random choices. The competitive-binding model outperformed the shuffled model for both binary–ternary mixtures (shuffled rmse = 10–100 times CB rmse; *SI Appendix*, Fig. S3*C*) and the 12-component mixtures (shuffled median rmse = 0.95 ∼ 6 times CB median rmse).

Extensions of the Model. So far, we have considered the simplest possible form of odorant–receptor interaction: Only one odorant molecule binds a receptor binding site at a time. Surprisingly, most of the receptors studied in our experiments were well described by this model. Competitive binding can produce essentially three types of nonlinear receptor responses to presentation of mixtures (Fig. 3 *A*–*C*): (*i*) domination by the odorant that gives the highest response individually (overshadowing, Fig. 3*A*), (*ii*) a response in between those to the individual odorants (suppression, Fig. 3*B*), and (*iii*) domination by the odorant that gives the lowest individual response (also called overshadowing, Fig. 3*C*). These effects can arise both from the intrinsic properties of the receptor–odorant interaction (difference in EC50) and/or due to extrinsic factors such as the ratio of concentrations. Such qualitative effects have been reported previously (14) in a phenomenological model that has a more complex form of response to mixtures. We have shown here that these effects can already be exhibited by a simple model directly rooted in biophysical competition between the odorant molecules seeking to occupy the receptor.

Our model can be easily extended to incorporate additional biophysical interactions that produce effects such as synergy (18) and inhibition (31). Although previous work (9, 13, 14) has explored possible mathematical functions that can be used to fit such nonlinearities in receptor response data, a biophysical understanding of the origin of these effects has been missing. Some recent progress on this front is reported by the authors of ref. 15 who focused on antagonism in receptors and proposed, e.g., additional interactions with cell membranes as a mechanism for nonspecific suppression. These authors also argued on theoretical grounds that antagonism can normalize receptor neuron population activities, improving the performance of decoders of the response ensemble. Our approach of starting from the simplest interactions at the molecular level provides an avenue for systematically identifying important interactions. For example, consider facilitation, where the binding of an odorant promotes the binding of other odorants to the same site. Such an interaction modifies Eq. **1** (*Materials and Methods* and *SI Appendix*, *Facilitation*) and produces effects such as synergy (Fig. 3*D*), in

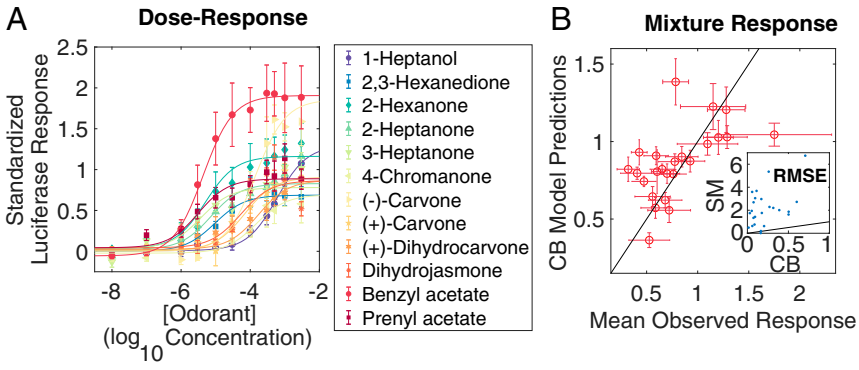

Fig. 2. A competitive binding model predicts olfactory receptor response to 12-component mixtures. (*A*) Response of receptor Olfr168 (mouse) to 12 individual odorants. Markers show mean experimental measurements ±1 SD. Solid curves show CB model. (*B*) CB model predictions vs. experimental responses for Olfr168. The error bars represent ±1 SD. (*B*, *Inset*) rmse of summation model (SM) plotted vs. the CB model. The black diagonal line is the unit slope line.

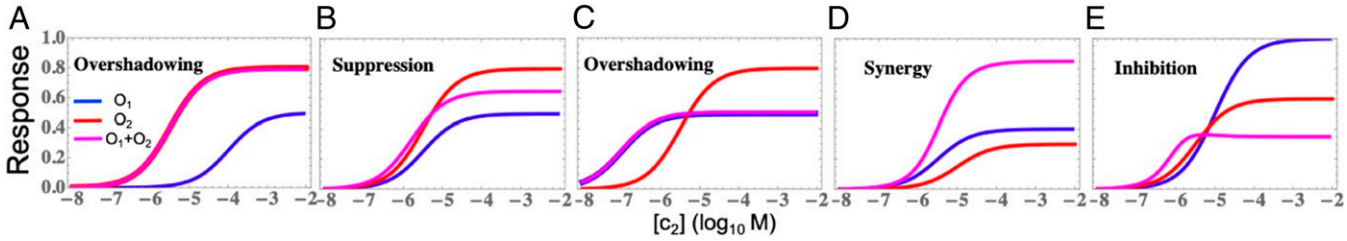

Fig. 3. (*A–C*) Phenomena exhibited by the competitive-binding model. The competitive-binding model with different parameter choices shows diverse effects for binary mixtures (purple) of two odorants (red and blue). Shown here are effects due to variations of *EC*50: (*A*) overshadowing by the odorant with the higher individual response ($EC50_1 = 10^{-4.0}$); (*B*) suppression, where the response is in between the responses of the individual odorants ($EC50_1 = 10^{-5.5}$); and (*C*) overshadowing by the receptor that produces the lower individual response ($EC50_1 = 10^{-7.0}$). Value of the other model parameters: $F_{max} = 1$, $e_1 = 0.5$, $e_2 = 0.8$, and $EC50_2 = 10^{-5.5}$. We assume equimolar mixtures ($c_1/c_2 = 1$). (*D* and *E*) Phenomena exhibited by the extended model including odorant facilitation. Facilitation of odorant binding by another odorant molecule in mixture leads to additional effects like synergy and inhibition. (*D*) Synergy: receptor response is higher than response to both the individual odorants. (*E*) Inhibition: response to mixtures is lower than the response to either individual odorant. Functional forms for facilitation and parameter choices leading to synergy and inhibition are given in *SI Appendix, Facilitation*.

which the response of the receptor is higher than the sum of the response to both individual odors, and inhibition (Fig. 3*E*) where the response is below the response to both individual odorants. This is in addition to the effects already produced by competitive binding (overshadowing and suppression, Fig. 3 *A–C*). Alternatively, if there are multiple independent binding sites for odorants, the mixture response will be the sum of the individual components (*SI Appendix, Independent binding sites*). More complex biophysical interactions, such as noncompetitive inhibition (*SI Appendix, Noncompetitive inhibition*), heterodimerization (*SI Appendix, Odorant dimerization*), catalysis by odor molecules, etc., can similarly be added to the basic model in a principled way.

To illustrate our proposed systematic approach to adding interactions, we considered the three receptors whose responses to binary and ternary mixtures deviated significantly from the predictions of the CB model (median rmse >0.1). For each of these receptors, we searched as follows for additional interactions between receptors and odorants. If the observed receptor responses were higher than the predictions of the CB model, we hypothesized a synergistic interaction. If the observed receptor responses were lower than the predictions of the CB model, we inferred the presence of suppression. We also looked at the composition of the mixtures for which the deviations were significant and identified the common odorant (if any) and incorporated an interaction with this odorant compensating for over- or under-predictions. The parameters of the extended CB model were chosen, similar to the CB model, by minimizing the root-mean-square error between observed response and predictions of the modified model weighted by the SD. Applying this procedure to the three remaining receptors significantly improved predictions (Fig. 4). Two receptors required inclusion of facilitative interactions (OR5P3, synergy between coumarin and acetophenone; Olfr1062, synergy between all three pairs), and one receptor (Olfr1104) required inclusion of suppression by eugenol (for functional forms and model parameters see *Materials and Methods* and *SI Appendix, Modified models*). Overall, the extended CB model (rmse mean = 0.10, median = 0.06) outperformed a summation model (rmse mean = 0.17, median = 0.16) and a shuffled model (rmse mean = 0.90, median = 0.86). These results predict specific odor–receptor interactions that can be tested experimentally.

Discussion

In this work, we showed that a minimal biophysical model of odorant–receptor interaction incorporating just the simplest possible nonlinearity, namely competition between molecules for the binding site, can successfully predict the responses of many mammalian odor receptors to complex molecular mixtures. This is surprising because noncompetitive interactions are common in pharmacology, but we nevertheless found that our simple model explains the majority of the experimental results. More general interactions between odorants and receptors can be easily added to our model, at the cost of additional parameters. For example, we showed that the nonlinearities implied by just competitive exclusion and facilitation are sufficient to produce diverse effects that have been previously reported in the perception of odor mixtures including synergy (18), overshadowing (17), suppression (32), and inhibition (31). These effects were thought to have a neural origin, but our results suggest that they may be driven partly by the biophysics of receptors.

Experimental studies of olfaction have largely focused on simple odors consisting of only one or two odorant molecules. However, natural odors are generally complex, containing hundreds of volatile components, with 3–40 being essential for the characteristic odor (30). Thus, to understand how olfactory circuits operate in naturalistic environments, models must account for complex sensory stimuli, as visual neuroscience has done for some time. A first step toward this goal is to understand how the receptors themselves respond to mixtures of many molecules. In

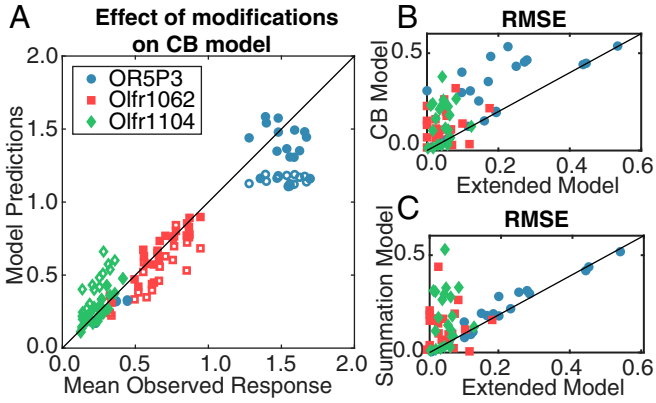

Fig. 4. Adding synergy and suppression improves predictions for three receptors. (*A*) The response of three olfactory receptors with the CB model (open symbols) and the extended CB model (solid symbols). Extensions: (*i*) OR5P3, synergy between coumarin and acetophenone; (*ii*) Olfr1062, synergy between all three pairs; and (*iii*) Olfr1104, suppression by eugenol. (*B*) rmse of the CB model vs. the extended CB model for the three receptors for each mixture. (*C*) rmse of the summation model vs. the extended CB model. In *A–C*, the black diagonal line is the unit slope line.

practical terms, the combinatorial explosion of the number of mixtures with different compositions means that the only hope for progress is to have a model that can predict mixture responses from dose–response curves, which can conceivably be measured for large panels of odorants in high-throughput experiments. Such a predictive model is most likely to be successful if it is rooted in the basic biophysics and biochemistry of molecular sensing, as our model is.

In olfaction, the low background activity of most receptors also makes it difficult to identify inverse agonists or antagonists using single molecules. But these effects, and more general noncompetitive interactions, do occur in mixtures. Fortunately, such interactions will typically involve small numbers of molecules as the probability of multiple molecules meeting to interact at the same time should decline exponentially with the number of interacting molecules. Thus, future studies should be able to explore the landscape of interactions by testing receptor responses to mixtures with just a small number of components.

We demonstrated a strategy to identify such interactions and used it to identify some receptors with suppressive and synergistic interactions. Note that this process of identifying interactions will converge efficiently only if we begin at a biophysically well-motivated starting point like our competitive-binding model. If we begin instead with an ad hoc model like linear addition of responses, many corrections will be needed to get a good description, as in the accumulation of epicycles required to describe simple elliptical orbits in the Ptolemaic model of the solar system. Even if we start with the competitive-binding model, the complexity of the added interactions must be discounted against the gain in accuracy, especially when including multiple interactions. This can be achieved via modern techniques in parametric statistical inference, e.g., ref. 33, that trade off model complexity against prediction accuracy.

In the study of color vision, models of the early visual system are combined with lookup tables of human responses to primary colors obtained through psychophysical experiments (34) to predict responses to arbitrary colors. These models have led to accepted industry standards that are used to produce color graphics through electronic or print means. Perhaps lookup tables of dose–response curves for olfactory receptors could be combined with models such as ours to predict responses to complex mixtures, ultimately allowing olfactory designers to create desired odors from a set of primary odorants.

Materials and Methods

See *SI Appendix* for detailed methods, biophysical models, and mathematical derivations.

Measurement of Dose–Response Curves and Mixture Response. Receptor responses were measured as luminescence of Firefly and *Renilla* reporters in a cell-based assay following the protocol for the Dual-Glo Luciferase Assay System (Promega) described in refs. 25 and 35. The enzyme is linear over seven orders of magnitude (36). In our system, luminescence from the firefly luciferase is a measure of receptor activity while luminescence from the *Renilla* luciferase measures how many cells are alive and successfully transfected. To measure receptor response, we first calculate the ratio of Firefly to *Renilla* luminescence on stimulation by the odor (*SI Appendix, Cell-based assay*). To standardize these measurements, we also measure the Firefly to *Renilla* luminescence ratio of a standard receptor (Olfr544) stimulated with nonanedioic acid at two concentrations (0 μM and 100 μM) under identical conditions. The luminescence ratio of the receptor is then divided by the difference between the luminescence ratios of the standard receptor at the two concentrations (*SI Appendix, Preprocessing*). This gives the standardized response of a receptor to the odor. Finally, we subtract the standardized response of the receptor at zero concentration of the odor to get the net response above baseline.

From 22 human and mouse receptors in ref. 26, we selected 18 responding to at least 2 of eugenol, acetophenone, and coumarin (Sigma-Aldrich). We measured the dose–response curves to these odorants at seven concentrations as well as a no-odor control. These seven concentrations spanned the total concentration range allowed in our assay (up to 0.3 mM), which is much higher than the biologically relevant concentrations found in the mucosa. We set a threshold for consistency that the difference between the standardized baseline response for a receptor to any pair of odorants should be within 0.2 of each other (see, e.g., the nearly overlapping baselines in Figs. 1*A* and 2*A* where this difference is nearly zero). Fifteen of the 18 receptors passed this test and were further stimulated with 21 mixtures (12 binary, 9 ternary) of eugenol, coumarin, and acetophenone (*Materials and Methods* and *SI Appendix*, Table S1) with concentrations selected to avoid receptor saturation.

From the data in ref. 26, we also identified one receptor, Olfr168, that was broadly tuned and for which dose–response curves were available for 12 odorants. We measured responses of this receptor to 24 mixtures of the 12 odorants and a no-odor control. Six mixtures contained all 12 odorants at equimolar concentrations. To select the other 18 mixtures, we first fitted our competitive-binding model to the dose–response data and used it to select pseudorandom concentrations of each odorant such that the predicted responses spanned the full dynamic range while avoiding saturation (compositions in *SI Appendix*, Table S3).

Model Parameter Estimation Using Dose–Response Measurements. For each odorant (i), we chose parameters ($EC50_i$ and the product $F_{max}e_i$) that minimize the root-mean-square error between the measured average response ($\bar{y}_{ex}(c_i)$) at concentrations c_i and the model predictions ($F(c_i)$), divided by the experimental SD (details in *SI Appendix, Model parameter estimation*); i.e.,

$$E_i = \sqrt{\frac{1}{M}\sum_{c_i}\left(\frac{(F(c_i)-\bar{y}_{ex}(c_i))}{\sigma(c_i)}\right)^2}. \quad [2]$$

$E_i < 1$ would mean that, on average, the model predictions lie within 1 SD away from the mean experimental observation. The minimization was performed using MATLAB *fminunc*. (Also see *SI Appendix, Dealing with unconstrained parameters* and *SI Appendix*, Fig. S5 and S6 for an alternative procedure for parameter estimation.)

Null Models. We considered a summation model where the receptor response to mixtures was a sum of the response to individual odorants at their concentrations in the mixture (*SI Appendix, Alternative models for comparison*). We also considered a shuffled model that has the same mathematical form as the competitive binding model (Eq. **1**), but with parameters chosen randomly with replacement from the set of dose–response parameters used in our analysis (57 sets; 45 sets from the 15 receptors of the binary–ternary analysis and 12 sets of the receptor Olfr168 from the 12-component analysis). Each parameter of the shuffled model is chosen independently. We report average prediction error (rmse) over 300 such random choices.

Competitive-Binding Model and Extensions. Mathematical derivation of the models from the biophysics of molecular binding is given in *SI Appendix*. The model for synergistic interaction (*SI Appendix, Facilitation*) has the form

$$F(c_1,c_2) = \frac{F_{max}\left(e_1\frac{c_1}{EC50_1} + e_2\frac{c_2}{EC50_2} + e_{12}\frac{c_1c_2}{EC50_{12}}\right)}{\left(1+\frac{c_1}{EC50_1}+\frac{c_2}{EC50_2}+\frac{c_1c_2}{EC50_{12}}\right)}, \quad [3]$$

where e_{12} and $EC50_{12}$ are the parameters of the interaction between the two odorants. The model with suppression (*SI Appendix, Noncompetitive inhibition*) has the form

$$F(c_1,c_2) = \frac{F_{max}\left(e_1\frac{c_1}{EC50_1} + e_2\frac{c_2}{EC50_2}\right)}{\left[1+\frac{c_1}{EC50_1}+\left(\frac{c_2}{EC50_2}\right)\left(1+K_1\frac{c_1}{EC50_1}\right)\right]}, \quad [4]$$

where K_1 is the suppression parameter for odor 1.

Data and Software Availability. Data and software are available from Open Science Framework (27).

ACKNOWLEDGMENTS. V.B. and V.S. were supported by the Simons Foundation (Grant 400425; Mathematical Modeling of Living Systems). V.B. was supported by US–Israel Binational Science Foundation Grant 2011058 and Physics Frontiers Center Grant PHY-1734030. Work by V.B. at the Aspen

Center for Physics was supported by NSF Grant PHY-1607611. N.R.M. and J.D.M. were supported by Grant R01 DC013339. A portion of this work was performed using the Monell Chemosensory Receptor Signaling Core and Genotyping and DNA/RNA Analysis Core, which was supported, in part, by funding from the US National Institutes of Health National Institute on Deafness and Other Communication Disorders Core Grant P30 DC011735.

1. Wandell BA (1995) *Foundations of Vision* (Sinauer Associates, Sunderland, MA).
2. Brainard DH, Stockman A (2010) Colorimetry. *The Optical Society of America Handbook of Optics, Vision and Vision Optics*, eds Bass M, et al. (McGraw Hill, New York), Vol 3, pp 10.1–10.56.
3. Nelson P (2017) *From Photon to Neuron: Light, Imaging, Vision* (Princeton Univ Press, Princeton, NJ).
4. Khan AG, Thattai M, Bhalla US (2008) Odor representations in the rat olfactory bulb change smoothly with morphing stimuli. *Neuron* 57:571–585.
5. Gupta P, Albeanu DF, Bhalla US (2015) Olfactory bulb coding of odors, mixtures and sniffs is a linear sum of odor time profiles. *Nat Neurosci* 18:272–281.
6. Kim AJ, Lazar AA, Slutskiy YB (2011) System identification of Drosophila olfactory sensory neurons. *J Comput Neurosci* 30:143–161.
7. Martelli C, Carlson JR, Emonet T (2013) Intensity invariant dynamics and odor-specific latencies in olfactory receptor neuron response. *J Neurosci* 33:6285–6297.
8. Ferreira V (2012) Revisiting psychophysical work on the quantitative and qualitative odour properties of simple odour mixtures: A flavour chemistry view. Part 1: Intensity and detectability. A review. *Flavour Fragrance J* 27:124–140.
9. Rospars JP, Lansky P, Chaput M, Duchamp-Viret P (2008) Competitive and noncompetitive odorant interactions in the early neural coding of odorant mixtures. *J Neurosci* 28:2659–2666.
10. Arnson HA, Holy TE (2013) Robust encoding of stimulus identity and concentration in the accessory olfactory system. *J Neurosci* 33:13388–13397.
11. Kundu S, Ganguly A, Chakraborty TS, Kumar A, Siddiqi O (2016) Synergism and combinatorial coding for binary odor mixture perception in Drosophila. *eNeuro* 3:ENEURO.0056-14.
12. Shen K, Tootoonian S, Laurent G (2013) Encoding of mixtures in a simple olfactory system. *Neuron* 80:1246–1262.
13. Cruz G, Lowe G (2013) Neural coding of binary mixtures in a structurally related odorant pair. *Sci Rep* 3:1–11.
14. Marasco A, De Paris A, Migliore M (2016) Predicting the response of olfactory sensory neurons to odor mixtures from single odor response. *Sci Rep* 6:1–12.
15. Reddy G, Zak JD, Vergassola M, Murthy VN (2018) Antagonism in olfactory receptor neurons and its implications for the perception of odor mixtures. *eLife* 7:e34958.
16. Oka Y, Omura M, Kataoka H, Touhara K (2004) Olfactory receptor antagonism between odorants. *EMBO J* 23:120–126.
17. Schubert M, Sandoz JC, Galizia G, Giurfa M (2015) Odourant dominance in olfactory mixture processing: What makes a strong odourant? *Proc R Soc Lond Ser B* 282:20142562.
18. Ishii A, et al. (2008) Synergy and masking in odor mixtures: An electrophysiological study of orthonasal vs. retronasal perception. *Chem Senses* 33:553–561.
19. Johnson KA, Goody RS (2011) The original Michaelis constant: Translation of the 1913 Michaelis–Menten paper. *Biochemistry* 50:8264–8269.
20. Johnson KA (2013) A century of enzyme kinetic analysis, 1913 to 2013. *FEBS Lett* 587:2753–2766.
21. Cornish-Bowden A (2015) One hundred years of Michaelis–Menten kinetics. *Perspect Sci* 4:3–9.
22. Wang ZX (1995) An exact mathematical expression for describing competitive binding of two different ligands to a protein molecule. *FEBS Lett* 360:111–114.
23. Collini M, et al. (2003) Competitive binding of fatty acids and the fluorescent probe 1-8-anilinonaphthalene sulfonate to bovine β-lactoglobulin. *Protein Sci* 12: 1596–1603.
24. Plette AC, Benedetti MF, van Riemsdijk WH (1996) Competitive binding of protons, calcium, cadmium, and zinc to isolated cell walls of a gram-positive soil bacterium. *Environ Sci Technol* 30:1902–1910.
25. Trimmer C, Snyder LL, Mainland JD (2014) High-throughput analysis of mammalian olfactory receptors: Measurement of receptor activation via luciferase activity. *J Visualized Exp JoVE* 88:51640.
26. Saito H, Chi Q, Zhuang H, Matsunami H, Mainland JD (2009) Odor coding by a mammalian receptor repertoire. *Sci Signal* 2:ra9.
27. Mainland J (2019) Competitive binding predicts nonlinear responses of olfactory receptors to complex mixtures. Open Science Framework. Available at https://osf.io/aj29q/. Deposited April 6, 2019.
28. Berglund B, Berglund U, Lindvall T, Svensson LT (1973) A quantitative principle of perceived intensity summation in odor mixtures. *J Exp Psychol* 100:29–38.
29. Grosch W (2001) Evaluation of the key odorants of foods by dilution experiments, aroma models and omission. *Chem Senses* 26:533–545.
30. Dunkel A, et al. (2014) Nature's chemical signatures in human olfaction: A foodborne perspective for future biotechnology. *Angew Chem Int Ed* 53:7124–7143.
31. Sanhueza M, Schmachtenberg O, Bacigalupo J (2000) Excitation, inhibition, and suppression by odors in isolated toad and rat olfactory receptor neurons. *Am J Physiol Cell Physiol* 279:C31–C39.
32. Simon TW, Derby CD (1995) Mixture suppression without inhibition for binary mixtures from whole cell patch clamp studies of in situ olfactory receptor neurons of the spiny lobster. *Brain Res* 678:213–224.
33. Balasubramanian V (1997) Statistical inference, Occam's razor, and statistical mechanics on the space of probability distributions. *Neural Comput* 9:349–368.
34. International Commission on Illumination (1986) *Publication CIE no. 15.2* (Central Bureau of the Commission Internationale de L'Eclairage, Vienna).
35. Zhuang H, Matsunami H (2008) Evaluating cell-surface expression and measuring activation of mammalian odorant receptors in heterologous cells. *Nat Protoc* 3:1402–1413.
36. Promega Corporation (2013) Measuring the Dual-Glo luciferase assay on the GLoMax discover system (Promega Corporation, Madison, WI), Application Note AN245.